FEATURE ARTICLE

Unimolecular Reaction of NO_2: Overlapping Resonances, Fluctuations, and the Transition State

Scott A. Reid[†] and Hanna Reisler*

Department of Chemistry, University of Southern California, Los Angeles, California 90089-0482

Received: September 25, 1995[⊗]

The unimolecular decomposition of expansion-cooled NO_2 at excess energies 0−3000 cm^{-1} is described with emphasis on the manifestations of overlapping resonances. When NO_2 is excited to energies above dissociation threshold, overlapping resonances interfere and give rise to final state-selected spectra which depend on the monitored final state of the NO product. The differences among the spectra diminish with the degree of incoherent superposition (e.g., thermal averaging). In this article, we describe the experimental manifestations of overlapping resonances in the case of barrierless unimolecular reactions and how they relate to transition state theories. We treat the unimolecular reaction of NO_2 using resonance scattering theory combined with random matrix formalism and distinguish between the near-threshold region where the transition state is loose and dissociation at higher excess energies where the transition state has tightened significantly. The final state-selected spectra and their dependence on the degree of resonance overlap are simulated in a qualitative way. Experimentally, fluctuations are observed in the line shapes, positions, and intensities in the spectra; the rotational and vibrational NO state distributions; the spin−orbit states of the oxygen atom correlated with specific quantum states of NO; and the state-specific rates. We show how the patterns of fluctuations in the rotational distributions allow the distinction between the loose and tight transition state cases and discuss the evolution of the excited complex from transition state to final products. In spite of the fluctuations, the averaged results agree well with the predictions of statistical theories, and implications for the transition state and the adiabatic evolution of the NO degrees of freedom are discussed. Even when the product state distributions agree with the predictions of specific statistical models, caution should be exercised in inferring properties of the transition state, due to the unaccounted influence of final state interactions beyond the transition state.

I. Introduction

Understanding the dynamics of unimolecular decomposition has been a long-standing goal of physical chemistry.[1−6] However, only in the recent past have experiments with good initial and final state selection become possible,[7−9] allowing detailed examination of the central assumptions of statistical theories as well as the unraveling of the underlying causes of statistical behavior. For small molecules it is possible to record well-resolved spectra in the region below dissociation threshold (D_0) and observe the appearance of quasibound states (or resonances) when coupling to the continuum occurs above D_0. Thus, the connection between resonance scattering and statistical behavior can be examined. It is the purpose of this article to describe such resonances in the unimolecular reaction of NO_2 and in particular to highlight the importance of *overlapping resonances* in understanding product state distributions (PSD's) and the evolution of the different internal degrees of freedom from reactants to products.

As a starting point, it is instructive to demonstrate that, except for the tunnelling regime or very near threshold, unimolecular reactions that can be described by statistical theories occur in the regime of overlapping resonances. The average rate of decay of isolated resonances $k(E)$ is related to the average width $\langle\Gamma(E)\rangle$ by

$$\langle\Gamma(E)\rangle = k(E)h/2\pi \tag{1}$$

We define the resonances as overlapping when their average width exceeds their average separation:

$$\langle\Gamma(E)\rangle > \Delta E \tag{2}$$

or, since $\Delta E = 1/\varrho(E)$, where $\varrho(E)$ is the density of states, we require that $\langle\Gamma(E)\rangle\varrho(E)$, which we term the overlap parameter, be ≥ 1. According to transition state theory (TST) and eq 1,

$$k(E) = N^{\dagger}(E)/h\varrho(E) = \langle\Gamma(E)\rangle 2\pi/h \tag{3}$$

where $N^{\dagger}(E)$ is the number of energetically open states of the transition state (TS). From here it follows that resonances overlap whenever

$$\langle\Gamma(E)\rangle\varrho(E) = N^{\dagger}(E)/2\pi > 1 \tag{4}$$

i.e., even when only few levels of the TS are open.

Why is it then that so little attention has been paid to the role of overlapping resonances in unimolecular reactions? The reason is that traditionally these reactions have been initiated by thermal activation, where the inherent averaging over a canonical ensemble of a dense manifold of states naturally

[†] Present address: Department of Chemistry, Marquette University, Milwaukee, WI 53233.

[⊗] Abstract published in *Advance ACS Abstracts,* December 15, 1995.

0022-3654/96/20100-0474$12.00/0

averages out effects due to overlapping resonances and interference. Thus, in chemistry attention has centered on classical descriptions involves the TS.[1−4]

In nuclear physics, the corresponding decomposition of a compound nucleus has been treated by statistical theories as well;[10] but since the numbers of initial and final states are typically much smaller than in molecular systems, the role of resonances has been emphasized from the outset. In fact, Niels Bohr, in his address to the Copenhagen Academy in 1936, discussed the broadening of the levels of the nucleus upon decomposition and added,[11] "This circumstance, together with the rapidly decreasing distance between neighboring levels in the energy region concerned, makes it indeed very likely that such levels will not here be separated at all...", resulting, of course, in overlapping resonances.

In the 1960s the role of overlapping resonances in nuclear and molecular statistical decompositions was explored in detail.[12,13] In nuclear physics, Ericson predicted that overlap between resonances and the ensuing interferences would cause spectra obtained for different final states to fluctuate with respect to line positions, shapes, and intensities. These predictions were later verified experimentally, and the phenomenon is known as "Ericson fluctuations".[14] Several methods for determining correlations among state-selected spectra were developed to estimate the randomness of the amplitudes and phases of the overlapping resonances.[15,16]

Work on resonances and interference in their couplings to the continuum inspired Mies and Krauss to apply the concept of overlapping resonances to unimolecular reaction rates.[17] Mies emphasized that great care must be exercised in extracting resonance parameters from spectra in the regime of overlapping resonances.[18] Mies and Krauss showed that, upon averaging over thermal initial conditions, interference effects were washed out, and the averaged rates agreed with the thermal rates obtained using statistical theories. Since no state-specific experimental results were available at that time, no attempt was made to treat state-selected spectra.

Recently, it has become possible to observe what we believe are experimental manifestations of overlapping resonances in a state-to-state unimolecular reaction. In this article we describe our studies of the decomposition of NO_2[19−23] and relate them to averaged results that can be compared with statistical theories.[1,2,6,24−26] When resonances overlap and interact via a common continuum, they interfere, and such interference will modify the line shapes and positions, giving rise to asymmetric line shapes commonly known as "Fano profiles".[27] Above D_0, partial absorption spectra can be obtained by monitoring specific final states of the products, the so-called photofragment yield (PHOFRY), photofragment excitation (PHOFEX), or action spectra. If the final states are uncorrelated, each may derive from a slightly different combination of resonance amplitudes and phases (for a fixed photolysis energy), giving rise to a somewhat different interference pattern and thus a different line shape. This is precisely what is observed in the state-to-state PHOFRY spectra of NO_2 and is the primary experimental indication of the presence of overlapping resonances.[20−22,28,29] Since effects due to interference tend to average out rapidly upon *incoherent* superposition, both the initial state of the parent molecule and the final state of the product must be well defined in order to observe these effects. This is best achieved with small (e.g., triatomic) parent molecules. However, to justify comparisons with statistical theories, the parent eigenstates must be ergodic, a condition that is not easily met for triatomic molecules. So far, NO_2 is the only triatomic molecule whose unimolecular reaction has been investigated and for which this condition is satisfied.

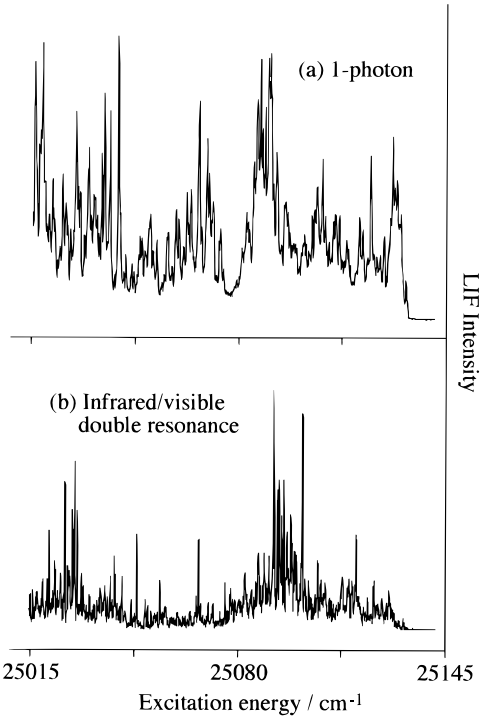

Figure 1. Fluorescence excitation spectra of jet-cooled NO_2 ($T_{rot} \sim 5$ K) in the region 0−120 cm^{-1} below dissociation threshold, obtained using (a) one-photon and (b) double-resonance IR−visible excitation (from ref 22). Note the reduction in spectral congestion achieved with double-resonance excitation.

The unimolecular reaction of NO_2 has been studies continuously as a function of excess energy:

$$NO_2(E^{\ddagger}) \rightarrow NO(^2\Pi_{\Omega};v;J;\Omega{=}1/2,3/2;\Lambda{=}A',A'') + O(^3P_j;\, j{=}2,1,0)$$

where Ω denotes the NO spin−orbit state, Λ the Lambda doublet state, and j the oxygen atom spin−orbit state. NO_2 exhibits both complete intramolecular vibrational redistribution (IVR) and well-resolved molecular eigenstates just below D_0.[28−31] Examples of $1^2B_2 \leftarrow 1^2A_1$ fluorescence excitation spectra of expansion cooled NO_2 in the region below D_0 obtained via one- and two-photon laser excitation are shown in Figure 1. Above D_0, resonances are created that are coupled to the continuum.[28,29] Each resonance has a characteristic width, and several resonances usually overlap. In addition, there is a well-known strong nonadiabatic interaction in NO_2 promoted by the asymmetric stretching mode which results in a conical intersection of the optically accessible $^2B_2$ and ground $^2A_1$ surfaces near the $^2B_2$ minimum.[32−40] This interaction gives rise to the extreme complexity of the NO_2 visible absorption spectrum and leads to vibronic chaos at excitation energies $>16\,000$ cm^{-1}, which is established in <200 fs following excitation.[31,40] It has been shwon that eigenstates in the vicinity of D_0 ($25\,130 \pm 2$ cm^{-1})[28,41,42] are predominantly of $^2B_2/^2A_1$ character, and each molecular eigenstate can be described as a linear combination of many zeroth-order wave functions with random coefficients.[32−40] Density of state considerations dictate that the molecular eigenstates have a predominantly ground state character, and it is well established that dissociation takes place on the ground electronic surface.[19,43−45]

To test predictions of statistical theories, both microcanonical unimolecular reaction rates and PSDs are needed. In TST the

rate is calculated by finding the dividing surface of minimum flux perpendicular to the reaction coordinate (the TS) for each excess energy $E^\dagger$. When an activation barrier exists, the dividing surface is usually located at the top of this barrier, and RRKM theory has proven very successful in calculating rates. PSD's in this case are largely controlled by the dynamics *beyond* the barrier, and their calculation requires detailed knowledge of the potential energy surface (PES) in this region. The situation is more complex for dissociation in the absence of an activation barrier, as is common when the products are free radicals. In this case, the location of the TS must be determined variationally at each $E^\dagger$.[4,6,24] Even the definition of the reaction coordinate is more subtle in this case.[46] It is now well established that the TS moves inward from atop the centrifugal barrier as $E^\dagger$ increases. This is physically interpreted as deriving from a subtle interplay between entropic and enthalpic factors, in which the former becomes more important at large $E^\dagger$, leading to a progressive tightening of the TS.[4,46] Thus, in a triatomic molecule the TS levels will resemble those of a free rotor at low $E^\dagger$ and be best described as hindered rotors or low-frequency bends at higher $E^\dagger$.

While rate calculations are rather straightforward even for a loose TS, the calculated PSD's must be examined more carefully. Near D_0, where the TS is very loose and its levels resemble those of the products, phase space theory (PST) becomes the natural choice. This theory apportions product populations as per the degeneracies of product quantum states, subject only to energy and angular momentum constraints. As the TS tightens (but a barrier is absent), the situation is less clear and the issue of adiabaticity beyond the TS arises; i.e., do product states still exchange energy beyond the TS? In other words, how important are exit channel interactions beyond the TS? The current view is that product vibrations, especially those of a diatomic fragment, evolve rather adiabatically.[8,9,24] Rotational and spin−orbit states usually have small energy separations; do these evolve adiabatically, and if so where along the reaction coordinate does this happen? What are valid tests for statistical behavior of PSD's? As we will discuss, fluctuations and oscillation patterns in the PSD's provide insights into these important issues.

NO_2 provides the opportunity to study unimolecular reactions from fully state-resolved microcanonical ensembles and from the point of view of resonance scattering theory. It enables removal of much of the averaging prevalent in larger molecules, thus revealing the state-to-state fluctuations inherent in any averaged quantity. As such, NO_2 truly stands at the crossroads between statistics and dynamics, allowing us to examine carefully the sources of the observed fluctuations, the assumptions commonly used in statistical theories, and our ability to draw mechanistic inferences from highly averaged data.

In the case of NO_2, we have observed fluctuations in the NO rotational and vibrational distributions, as well as in the relative populations of the oxygen spin−orbit states correlated with a single NO quantum state. We also have indications that the rates from adjacent resonances fluctuate. We are able to qualitatively rationalize our results with a model that is based on the assumptions of statistical theories; namely, (i) the initial parent states are ergodic, and (ii) formation and decomposition of the activated complex are separated in time.

The unimolecular reaction of NO_2 has been studied extensively over the past 20 years,[19−23,28,29,41−61] and it is not the purpose of this article to provide an exhaustive review of these thorough and detailed investigations. Rather, we concentrate on experimental manifestations of overlapping resonances and their relation to statistical descriptions of the unimolecular reaction. Evidence of the statistical nature of the decomposition has been provided by both rate measurements and PSD's. The decomposition rates [$k(E)$], determined both at 5 and 300 K, agree reasonably well with RRKM or PST predictions near threshold and with variational RRKM theory at higher excess energies ($E^\dagger < 1400$ cm^{-1}).[43−45] In our own studies, carried out at excess energies $E^\dagger = 0-3030$ cm^{-1}, we find that NO rotational state distributions are well fit, *on average*, by PST, although significant fluctuations and oscillations exist about the PST predictions.[19−23] As usual, the vibrational distributions are "hotter" than predicted by PST but agree with variational RRKM calculations.[19,45,60,61] The decomposition can be described as proceeding via a loose, PST-like, TS near threshold, with the TS tightening progressively as $E^\dagger$ increases. Although experiments have been conducted at excess energies higher than 3000 cm^{-1}, the dissociation lifetime becomes very short ($\ll$1.0 ps), and thus the justification for treating the decomposition statistically becomes questionable.

II. Probes of Interferences among Overlapping Resonances in NO_2 Decomposition

A. State-Selected Photofragment Yield (PHOFRY) Spectroscopy. Our primary probe of interferences among overlapping resonances in NO_2 is photofragment yield (PHOFRY) spectroscopy. In this method, NO_2 molecules are optically excited to energies in excess of D_0, and nascent NO fragments are then detected via laser-induced fluorescence (LIF). Final state-selected PHOFRY spectra of NO_2 are obtained by scanning the photolysis laser frequency while probing a specific quantum state of the NO fragment. These "partial" absorption spectra reflect probabilities for both absorption and dissociation into the monitored NO state. The interference effects from overlapping resonances are manifested as a marked NO final state dependence of the width, shape, position, and the amplitude of spectral features.

Interference effects resulting from *coherent* superpositions (e.g., overlapping levels excited coherently) are diminished by *incoherent* superpositions resulting, for example, from thermal congestion. If more than one NO_2 rotational level is populated, the observed PHOFRY spectrum is an incoherent superposition of spectra from different initial levels. Parent state selection is typically attained via expansion cooling,[62] as used for example by Robra *et al*. and Miyawaki, *et al*., who obtained state-selected PHOFRY spectra of NO_2 near dissociation threshold.[28,29] Our approach combines jet cooling with double-resonance IR−visible excitation,[20,22] where specific rotational states in the (101 ← 000) band of NO_2 are excited with tunable infrared radiation from a $LiNbO_3$ optical parametric oscillator (OPO), and the vibrationally excited molecules are further excited with a tunable laser to energies above D_0. IR−visible PHOFRY spectra are obtained by scanning the photolysis wavelength for fixed IR and probe wavelengths. Information on thermal averaging is obtained by comparing IR−visible spectra to those obtained via single-photon excitation under similar experimental conditions.

We have also carried out calculations intended to demonstrate in a simple way the effects of coherently excited overlapping resonances on PHOFRY spectra in two distinct energy regimes.[22] First, we examine energies near D_0 where the results of Robra *et al*.[28] and Miyawaki *et al*.[29] were obtained. In this energy region the TS is loose, and its levels are approximately NO free rotor states (neglecting excited NO, O spin−orbit states). We then examine dissociation at $E^\dagger$ of several hundred to several thousand cm^{-1}, where the average degree of level overlap is more severe; here, the TS has significantly tightened, and its levels are best described as bending vibrations.[44,45]

The model described here is based on assumptions inherent in statistical theories; i.e., the parent eigenstates are ergodic, and the formation and decay of the activated complex have uncorrelated phases. Consequently, we assume that the parent level spacings are described by a Wigner-like distribution.[31,36,40] Since the parent wave functions can be described with a basis set of normal modes with random coefficients, we also assume that, in analogy with the case of isolated resonances, the coupling matrix elements to the continuum of fragment channels are random and that this, in turn, leads to randomly fluctuating decay widths obeying a chi-square distribution.[9,63−67] Thus, the amplitudes of the resonances, $R_m(E)$, are given by[14,63,68]

$$R_m(E) = \frac{a_m}{(E - E_m) + (i\Gamma_m/2)} \tag{5}$$

where E_m is the resonance energy, a_m is the resonance excitation coefficient, and Γ_m is the sum of the partial widths of the resonance m into all final channels f. In the case of isolated resonances, Γ_m can be measured directly from the line width and is related to the decay rate $k(E)$ by the uncertainty principle (eq 1). In contrast, when the resonances overlap, the decay width is an unobservable quantity, and the relationship between $\langle\Gamma(E)\rangle$ and $k(E)$ is not simple.[64,65] At each energy E, excitation is simulated (using the Franck−Condon principle and the dipole approximation) as coherent excitation of quasi-bound states with a random (Wigner-like) distribution of nearest-neighbor level spacings and having a random (chi-square-like)[66,67] distribution of decay widths. This is the starting point for both the loose and tight TS cases. We then need to project these resonances into fragment states in order to simulate the PHOFRY spectra. It is here that treatments of the loose and tight TS cases differ, as described below. We note that a more elaborate model, based on random matrix formulation of the Feshbach optical potential, has recently been applied to the same problem with similar results[64,65] and is described briefly in section II.C.

A.1. The Case of a "Loose" TS: Near-Threshold Dissociation of NO_2. In the loose TS limit (i.e., near D_0), the levels of the TS look like fragment states. Thus, the partial spectra are simulated by assuming that scattering of the overlapping resonances into each final state can be described by complex matrix elements with random amplitudes C_{fm} and phases ϕ_{fm}.[22] Interference occurs when the matrix elements deviate from the real axis, and each final state derives from a slightly different weighting of the overlapping resonances. This case is analogous to "Ericson fluctuations" in nuclear physics.[14] We write the cross section for formation of a specific pair of NO + O final states (denoted f) from initial parent state i as

$$\sigma_{f\leftarrow i}(E) = |\sum_m R_m(E)\, C_{fm} e^{i\phi_{fm}}|^2 = \left|\sum_m \frac{a_m C_{fm} e^{i\phi_{fm}}}{(E - E_m) + (i\Gamma_m/2)}\right|^2 \tag{6}$$

We use preselected arrays of E_m, a_m, and Γ_m, while C_{fm} and ϕ_{fm}, which define the projection of resonance m onto final state f, are changed for each f. The distribution of phases is assumed to be uniformly random, and the number of resonances within the chosen energy window is consistent with the average level density of NO_2 at that energy.[30,31,40] The coefficients a_m are chosen as uniform random deviates between 0 and 1.[68] Each quasi-bound level is explicitly assigned a decay width Γ_m, randomly chosen from a chi-square distribution with N degrees of freedom,[66,67] where N is the number of independent decay channels [i.e., $N = N^\dagger(E^\dagger)$]. In the simulations shown here, we assume that eq 3 is valid (but see section II.B) and relate N, ρ and $\langle\Gamma(E)\rangle$ by[64]

$$\langle\Gamma(E)\rangle = \frac{hk(E)}{2\pi} = \frac{N^\dagger(E^\dagger)}{2\pi\rho} = \frac{N}{2\pi\rho} \tag{7}$$

In the limit of a loose TS, $N^\dagger(E^\dagger)$ is counted according to phase space theory (PST), i.e., as the number of product states. Once a set of resonances is defined (i.e., arrays of E_m, A_m, and R_m are chosen), these parameters are fixed as inputs, while ϕ_{fm} and C_{fm} are chosen as uniform random deviates in the intervals $0-2\pi$ and $0-1$, respectively, and are changed for each calculation, i.e. for each f. Sequences of random deviates are generated via published algorithms.[69]

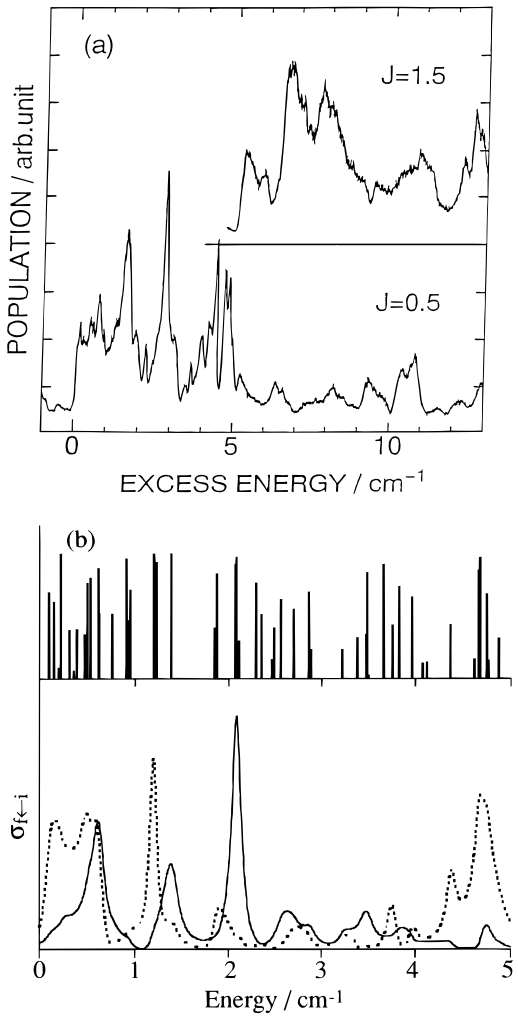

Figure 2. (a) Near-threshold PHOFRY spectra of NO_2 obtained by Miyawaki et al. (ref 29) for two rotational states ($J = 0.5$ and 1.5) of NO($^2\Pi_{1/2}$). (b) Calculated spectra simulating the region $0-5$ cm^{-1} above D_0, as described in the text. The positions and relative intensities of the underlying resonances used in the calculations are shown in the upper panel.

Shown in Figure 2a are two PHOFRY spectra obtained by Miyawaki et al. in the region $0-5$ cm^{-1} above threshold by monitoring the $\Pi(A')$ Λ-doublet state of NO($^2\Pi_{1/2}$; $J = 0.5$ and 1.5)[29] while Figure 2b displays two simulated PHOFRY spectra for this region calculated as described above; the upper panel shows the positions and relative intensities of the excited resonances. The density of quasibound levels assumed in the calculations reflects that observed in LIF spectra in the region $0-5$ cm^{-1} *below* threshold.[30,31] To account for electronic degeneracies of the fragments,[29] we set $N = 4$ in eq 7 and obtain $\langle\Gamma(E)\rangle\rho = 0.64$.

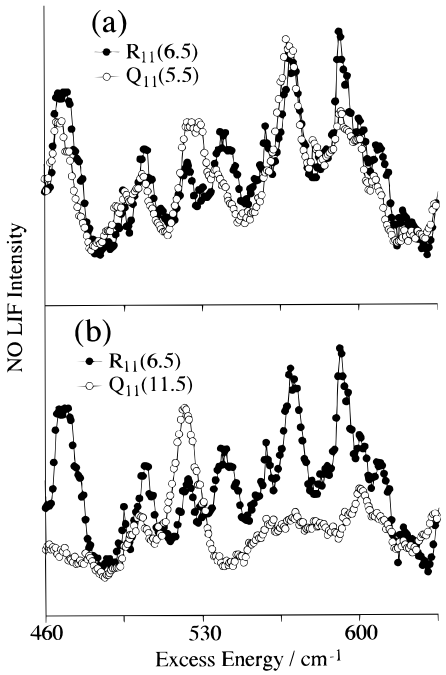

Figure 3. IR−visible PHOFRY spectra of NO_2 at $E^\dagger = 460-650$ cm^{-1} obtained for (a) two adjacent rotational states ($J = 6.5$ and 5.5) of NO($^2\Pi_{1/2}$) and (b) levels of significantly different J (11.5 vs 6.5). A much poorer correlation of spectral features is observed in (b) than in (a). (From ref 20.)

Comparing parts a and b of Figure 2, we see that qualitative features of the experimental PHOFRY spectra are reproduced in the calculated spectra. In both spectra the number of observed peaks is significantly smaller than the number of underlying quasi-bound levels (i.e., ∼10 vs 50). More importantly, spectra for different final channels clearly display different resonance structures. This effect is a signature of interferences among coherently excited overlapping resonances and a trademark of all state-selected PHOFRY spectra obtained for NO_2. It is intriguing that these effects are prominent so close to threshold, where the degree of overlap is modest (i.e., $\langle\Gamma(E)\rangle\rho \sim 1$). It reflects the fact that when N is small the distribution of decay widths is broad and that for randomly spaced resonances there are usually some regions of greater overlap.

A.2. A Tightening TS: Dissociation of NO_2 at $E^\dagger = 400-3000$ cm^{-1}. As the excess energy increases (e.g., $E^\dagger$) > 400 cm^{-1}), the decomposition changes in several ways: the dissociation rate increases, the *reactive* density of states decreases, and the TS progressively tightens. Since $\langle\Gamma\rangle$ increases, we might expect more levels to overlap on the average and interference effects to become more prominent. However, initially the increase in $\langle\Gamma\rangle$ is partially offset by a decrease in the density of *reactive* levels with increasing energy. This effect, discussed in detail elsewhere,[30,70] occurs when the time scale for decomposition becomes shorter than characteristic time scales for IVR. Simply stated, when an optically bright state is coupled more strongly to the continuum than to a subset of dark states, these dark states are excluded from the manifold of dissociative states. In unimolecular reactions, with increasing $E^\dagger$ coupling to the continuum becomes stronger than relatively weak *rovibronic* perturbations such as Coriolis and spin−rotation couplings,[30] and a transition is observed from a *rovibronic* to *vibronic* density of reactive states.

Evidence for this effect is found in IR−visible PHOFRY spectra at $E^\dagger = 475-650$ cm^{-1}. Here the average decay width (∼4 cm^{-1})[44] is an order of magnitude larger than typical NO_2 rovibronic coupling matrix elements (∼0.3 cm^{-1}).[71] Unlike the near threshold PHOFRY spectra where two rotational states of NO($^2\Pi_{1/2}$), $J = 0.5$ and 1.5, gave rise to different resonance structures,[29] the spectra obtained here for levels of adjacent J's exhibit *similar* resonance structures (Figure 3a). Only when probing levels of significantly different J (Figure 3b) do differences in the spectral features become apparent. Although the average decay width here is significantly larger than near threshold, the interference effects are not more prominent, since $\langle\Gamma(E)\rangle\rho$ is still small. This effect is also related to the significant tightening of the TS at these energies, as discussed below.

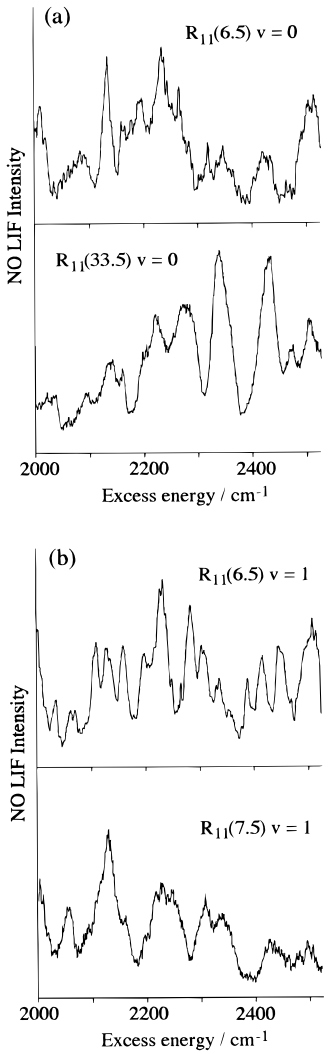

Figure 4. (a) IR−visible PHOFRY spectra of NO_2 at $E^\dagger = 2000-2500$ cm^{-1} obtained by monitoring two rotational states ($J = 6.5$ and 33.5) of NO($^2\Pi_{1/2}$;v=0) of very different J. Note the marked differences in spectral features. (b) Same as (a), but for NO(v=1) levels of similar J (6.5 vs 7.5).

Effects due to more severe level overlap become significant, however, at yet higher excess energies. We have closely investigated the region $E^\dagger = 2000-2500$ cm^{-1}, where the average decay width has increased to ∼15−20 cm^{-1},[26g,43,45] and $\langle\Gamma(E)\rangle\rho > 3$. Figure 4a displays two IR−visible PHOFRY spectra in this region for NO(v=0) levels of significantly different J. Consistent with spectra at lower $E^\dagger$, markedly different spectral features are observed. However, here the spectra obtained for levels of *similar j* also exhibit marked differences, as illustrated in Figure 4b. In fact, *all* IR−visible PHOFRY spectra obtained in the higher energy region exhibit pronounced differences in peak positions, shapes, widths and amplitudes. We have previously developed a quantitative measure of correlation, the correlation index, which supports

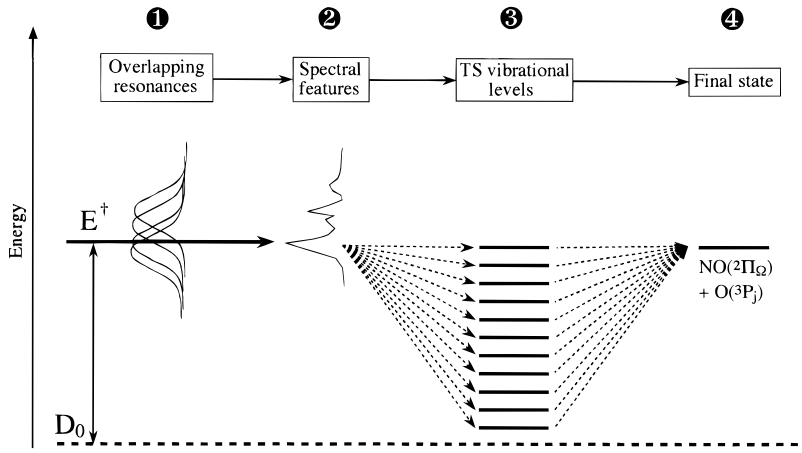

Figure 5. Schematic of the NO_2 dissociation mechanism. At a specific $E^\dagger$, several overlapping resonances are coherently excited (1) and (randomly) projected onto the energetically accessible levels of the tight TS (3). The TS levels, in turn, map onto specific sets of NO + O quantum states (4). Interaction among overlapping resonances and projection through multiple TS levels gives rise to interference resulting in different spectral features (2) for each monitored final state.

this conclusion.[21,22] As demonstrated by the calculations described below, this results from the larger degree of level overlap in the higher energy region.

In extending the model presented above to higher energies, we note that NO free rotor states no longer provide a good approximation to the TS levels, which now resemble more the hindered rotational or bending vibrational levels of an ON−O complex. Our model still assumes that evolution of the overlapping resonances to TS level n can be described by random complex coefficients, $C_{nm}e^{i\phi_{nm}}$. However, we now need to include also *dynamical* matrix elements, D_{fn}, to describe the evolution of the system from TS level n to product f:

$$\sigma_{f\leftarrow i} = |\sum_{m,n} D_{fn} C_{nm} e^{i\phi_{nm}} R_m|^2 \qquad (8)$$

This model, represented schematically in Figure 5, assumes that the populations of the energetically available TS levels are described as per eqs 6 and 7 with n substituted for f. Note that a similar expression combining statistics and dynamics has been more rigorously derived using an extension of the Feshbach optical model to include dynamical matrix elements beyond the TS (see section II.C).[65] We will illustrate the salient features of our model by using two separate sets of calculations describing (i) the evolution of coherently excited overlapping resonances up to the TS and (ii) the evolution of randomly populated TS levels to final products. The second calculation will be described in section II.D. Here we examine the effects of increasing overlap on part (i) by using eq 6, substituting n for f, thus simulating the projection of coherently excited overlapping resonances onto each level of the TS. While not accounting for the passage from TS to products, and thus additional interference and/or correlations which may result from decay via multiple TS levels (see section II.D), this calculation serves to illustrate qualitative changes in the PHOFRY spectra resulting from the combined effects of reduced density of reactive levels and larger $\langle\Gamma(E)\rangle$.

Shown in parts a and b of Figure 6 are pairs of synthetic PHOFRY spectra calculated using $\langle\Gamma\rangle\rho = 1$ and 3 for the regions corresponding to $E^\dagger = 475-650$ cm^{-1} and $E^\dagger = 2000-2500$ cm^{-1}, respectively. Experimental and theoretical estimates of $\langle\Gamma\rangle$ and the number of transition state levels N were used.[22] In order to simulate effects due to thermal averaging, three separate samplings were averaged for each spectrum (see below).[22] Remember that experimental PHOFRY spectra in these two energy regions exhibit pronounced differences. In the lower

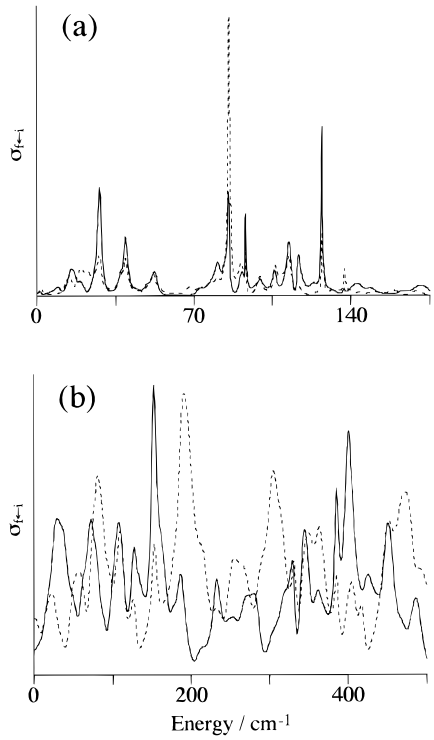

Figure 6. (a) Calculated spectra simulating PHOFRY spectra in the region $E^\dagger = 475-650$ cm^{-1}. (b) Same as (a), but for the region $E^\dagger = 2000-2500$ cm^{-1}. These spectra demonstrate the effects of increased level overlap on PHOFRY spectra. See text for details.

energy region a correlation is observed on the basis of J; a poorer correlation on this basis is observed at higher energies. Comparing the spectra within each pair in Figure 6, we indeed see the increased effect of overlap and interference on widths, shapes, and positions of the spectral features in Figure 6b.

Thus, our simulations are capable of reproducing the qualitative features of the PHOFRY spectra in the limits of both loose and tight TS. Before describing the dynamical evolution of the tight TS system beyond the TS, we will examine some of the assumptions made thus far, as well as effects of thermal averaging on the PHOFRY spectra.

B. A Transition-State-Based Random Matrix Model for Overlapping Resonances. Recently, Peskin *et al*. applied a random-matrix version of Feshbach's optical model (based on an effective potential formalism) to unimolecular reactions.[64,65] The model is useful when accurate PES's are unavailable and

exact dynamical calculations are beyond reach. It simulates average unimolecular decay rates in the regimes of isolated and overlapping resonances, and its interpretation is consistent with TST. Since the final state-selected spectra may depend also on the evolution of the system beyond the TS, the standard optical model has been modified by introducing "dynamical" coupling matrix elements. The mixed approach combines a universal statistical description of the molecular complex with a reaction-specific dynamical description of the propagation from TS to products. A clear advantage of the random-matrix/optical potential model is that it yields the distribution of decay widths and phases, and thus the assumptions made in the simplified model described here can be tested.

As in TST and in the simulations described here, the model assumes that the basis states, i.e., the molecular eigenstates in the absence of coupling to the continuum, are ergodic and have a Wigner distribution of nearest-neighbor level spacings and that all open channels are independently coupled to the basis states. The coupling matrix elements between each final state $|f,E\rangle$ and initial state $|i\rangle$, i.e. $v_{fi} = \langle f,E|H|i\rangle$, are taken to be real and energy independent in the selected (narrow) spectral range. They are chosen from a Gaussian (normal) distribution with standard deviation σ and a mean value 0, such that the average width $\langle\Gamma\rangle$ is given by

$$\langle\Gamma\rangle = 2\pi\sigma^2 N \tag{9}$$

where N is the number of final independent decay channels. In the TST interpretation of the optical model, the number of states independently coupled to the zeroth-order levels is identified with the numebr of energetically accessible states of the TS, and thus $\langle\Gamma\rangle$ is proportional to the number of open levels of the TS. For a loose TS, N is equal to the number of open fragment channels, and the probability of producing a final state f as a function of energy is given (as in eq 6) by the general form[65]

$$P_f(E) = \left|\sum_m \frac{a_m C_{fm} e^{i\phi_{fm}}}{(E - E_m) + (i\Gamma_m/2)}\right|^2 \tag{10}$$

where the real amplitudes C_{fm} and phases ϕ_{fm} are obtained directly by diagonalizing the effective Hamiltonian matrix. The diagonalization yields eigenvectors with (complex) eigenvalues $\{E_m - i\Gamma_m/2\}$. For a loose TS, $P_f(E)$ depends only on the effective Hamiltonian matrix and not on any specific exit channel dynamics. The state-selected spectra are obtained by calculating $P_f(E)$ as a function of E. Since as in TST, $\langle\Gamma\rangle$ (and hence the resonance overlap) increases with N, it also increases with E. The calculated spectra and their dependence on the monitored final state and on E are qualitatively similar to those obtained by the simplified method described in section II.A.1.

Furthermore, the calculations show that when the degree of overlap is small, the decay width distributions are well described as chi-square-like with N degrees of freedom. As the overlap increases, not only does the average width increase but also the distribution of widths increasingly deviates from a chi-square-like shape; its peak shifts toward smaller widths, while the larger widths extend farther than predicted by a chi-square distribution. Nonetheless, the qualitative behavior of the final state-selected spectra is insensitive to the exact form of the distribution of decay widths, and thus the use of a chi-square distribution in calculating the spectra shown in Figures 2b and 6 is reasonable.

The shapes of the spectral features are directly related to interference among overlapping resonances, which is characterized by their phases. Thus, it is instructive to obtain the phase distributions from the optical model and compare them with the random distribution assumed in the simulations above. It is found that when the overlap is very weak, the phases are strongly peaked around integer multiplies of π, indicating that the coefficients $C_{fm}e^{i\phi_{fm}}$ in eq 10 are approximately real.[65] As the coupling increases, the coefficients become more complex, and the phases quickly become uniformly and randomly distributed between 0 and 2π, as assumed in our simulations. Thus, the assumption of random phases commonly used in statistical theories is seen to be justified at all energies except near threshold where the degree of overlap is very small.

Although in the work of Peskin *et al*. the evolution of the system of resonances is treated as a scattering process, the physical interpretations are couched in terms of statistical TSTs.[64,65] In particular, the resonances are assumed to evolve to final products via the conventional TS. The main approximation of the model presented in refs 64 and 65 is the use of random matrix formalism that describes the coupling matrix elements between the molecular eigenstates and the continuum as statistically random, i.e., obeying a Gaussian (normal) distribution. For real molecules the coupling matrix elements are molecule- and state-specific and may be correlated, especially for adjacent resonances or energetically close final channels. Thus, in the actual unimolecular reaction of NO_2 some dynamical features may be manifest. When state-specific effects are not important (i.e., on the average), random fluctuations about the statistical expectations are expected in the case of a loose TS and moderate resonance overlap.

Finally, we point out that Peskin et al. have recently shown that when resonances overlap, the average width cannot be linearly related to the average rate simply by the uncertainty principle, but in fact the calculated rate is always smaller than that inferred from the average width.[64,65] Thus, eq 7 cannot be rigorously used, and $\langle\Gamma(E)\rangle$, ρ, and N should be treated as independent parameters. The qualitative behavior of the simulated spectra, however, does not depend sensitively on this relation, since the critical parameter is the overlap parameter, $\langle\Gamma(E)\rangle\rho$.[72]

C. Effects of Thermal Averaging: One-Photon PHOFRY Spectra. The state-selected IR−visible PHOFRY spectra demonstrate that the degree of overlap is important in determining the shapes of spectra and correlations among spectra obtained for different final states. Also important is the degree of thermal averaging, since we expect *incoherent* superpositions to dampen, or even completely wash out, interference effects. To investigate experimentally this effect, we have obtained a series of *one-photon* PHOFRY spectra under identical conditions. A direct comparison of IR−visible and one-photon PHOFRY spectra is not possible due to different selection rules for the two excitation schemes (see Figure 1);[22] we therefore base our comparison on correlations within each set of spectra. The main difference between the two experiments is that the number of initial parent rotational levels accessed is significantly reduced in the double-resonance experiments.[22]

Figure 7 displays pairs of one-photon PHOFRY spectra at $E^\dagger = 2150-2450$ cm^{-1} obtained for NO levels of similar J. The spectra in each pair exhibit almost perfect correlation of the spectral features. Note, however, that different features are observed when comparing the different pairs of spectra and thus levels of very different J. This illustrates the pronounced correlation between levels of similar J observed in one-photon PHOFRY spectra in this energy region.[21] This correlation is not seen in IR−visible spectra in this region (see Figure 4b),[22] nor in fact do any pairs of IR−visible spectra display the level

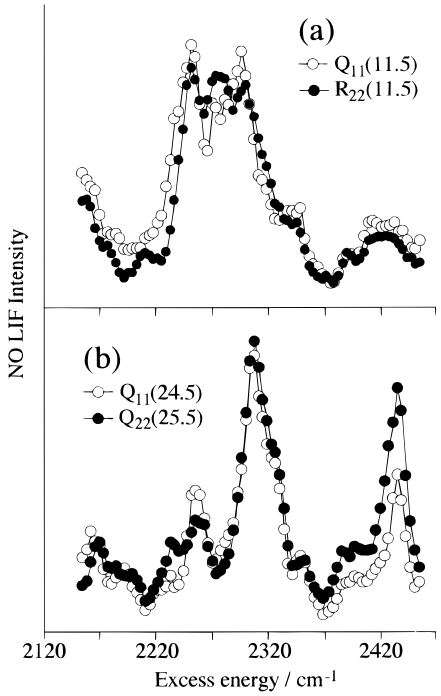

Figure 7. One-photon PHOFRY spectra at $E^{\dagger} = 2150-2450$ cm^{-1} obtained (a) for two rotational states of NO(v=0) of the same J (11.5) and (b) for levels of significantly higher J (24.5 vs 25.5). These spectra (from ref 21) reveal a pronounced correlation on the basis of J.

of correlation observed in Figure 7. The correlation indices for these spectra support this conclusion.[21,22]

A second difference between state-selected and one-photon PHOFRY spectra concerns the resonance widths. IR−visible PHOFRY spectra obtained at $E^{\dagger} = 2000-2500$ cm^{-1} *routinely* display spectral features narrower than 25 cm^{-1} (fwhm) and as narrow as 3 cm^{-1}.[22] In contrast, one-photon PHOFRY spectra *rarely* display features narrower than 25 cm^{-1} and none narrower than ∼15 cm^{-1}.[21] Note that at these energies the average decay width (∼15−20 cm^{-1})[26g,43,45] is significantly larger than the rotational envelope of a vibronic band (∼5 cm^{-1}) at the characteristic rotational temperature of our experiment, ∼5 K.[39] Excitation from different parent rotational levels thus accesses primarily the same set of overlapped vibronic levels, with relative excitation probabilities determined by line strength factors. Excitation from each parent rotational level *coherently* accesses these levels, and interferences produce specific spectral structures; however, the weightings of the resonances may be slightly different for different initial states, resulting in somewhat different spectra. Since excitation from different parent rotational levels is incoherent, the observed spectrum will be a superposition, displaying broader structures. This could explain why a greater number of narrow features are observed in IR−visible spectra and account in part for the lack of correlations in these spectra. A similar type of broadening is exhibited when PHOFRY spectra obtained by monitoring O(^{3}P$_j$) states are compared to those obtained by monitoring NO($^2\Pi_\Omega$,v,J,Λ) states. Each O(^{3}P$_j$) spectrum is in fact a superposition of many spectra correlated with the open NO channels and thus exhibits much broader spectral features.[52] Thus, in the case of overlapping resonances the widths of features in the total absorption spectrum are usually broader than in the state-selected spectra. Simulations show that when many state-selected spectra are summed, the resulting spectrum becomes similar to that obtained by simple incoherent superposition of the individual underlying resonances.[72] Thus, the regime where the random phase approximation is applicable is rapidly approached when summing over initial and/or final states.

In conclusion, by comparing correlations in IR−visible and one-photon PHOFRY spectra, we show that even modest thermal averaging significantly dampens interference effects; this partially explains why such effects are not commonly observed. We also demonstrate that the degree of level overlap is important in governing the magnitude of these effects.

D. NO Product State Distributions: Mappings of TS Wave Functions. Additional insights into overlapping resonances and the unimolecular reaction mechanism are obtained by examining PSD's. Although the PHOFRY spectra and NO product state distributions are complementary ways of viewing the same information, the latter sometimes better reveal patterns and regularities. We have obtained complete (i.e., rotational, vibrational, and spin−orbit) state distributions of the nascent NO fragment for dissociation at specific excess energies in the range $E^{\dagger} = 0-3038$ cm^{-1}.[19,23] In these experiments the excitation laser wavelength is fixed at a given $E^{\dagger}$ and the probe laser wavelength then scanned to record the complete NO rovibrational spectrum, from which the distributions are extracted.[19] In this section we examine how the correlations and fluctuations observed in PHOFRY spectra are manifest in the NO PSD's. In section III we compare the PSD's with statistical predictions and examine the implications of the observations to the dissociation mechanism, especially in the TS region.

We focus here on NO rotational state distributions, since a correlation based on J has been observed in the PHOFRY spectra, and again separate our results into regimes of excess energy near and significantly above D_0. Displayed in Figure 8 are NO($^2\Pi_{1/2}$,v=0) rotational distributions obtained using IR−visible excitation at $E^{\dagger} = 235$ and 400 cm^{-1}. The distributions for the two (A′,A″) Λ-doublet states of NO($^2\Pi_{1/2}$) are shown, as well as a semilog plot of the distribution summed over Λ-doublet levels and compared with PST calculations. Inspection of each Λ-doublet level distribution reveals fluctuations in the rotational populations; in addition, the relative Λ-doublet populations for each J fluctuate considerably as a function of J. The fluctuations are significantly diminished, however, when summing over the Λ-doublet levels. These observations are characteristic of NO rotational state distributions at $E^{\dagger} = 0-400$ cm^{-1} and are consistent with the near-threshold PHOFRY spectra.[28,29]

Shown in Figure 9 (following the format of Figure 8) are NO($^2\Pi_{1/2}$,v=0) rotational distributions obtained using one-photon excitation at $E^{\dagger} = 2061$ and 3038 cm^{-1}, respectively. Here, the distributions show pronounced oscillatory structures which are well reproduced for the two Λ-doublet states, as well as for spectra obtained when monitoring NO($^2\Pi_{3/2}$) (see Figure 10), and therefore are not diminished upon summation of all fine-structure states. However, they are very different for the two excess energies. The regular oscillatory structures are more easily identified in distributions obtained via one-photon excitation, since fast fluctuating structures are averaged out by incoherent superpositions of distributions correlating with several parent rotational states. Recall that at higher $E^{\dagger}$ the TS levels resemble hindered rotational or bending vibrational levels of an ON−O complex, so that our picture of the decomposition now includes projections of the excited resonances onto the final state manifold *via the TS* (see Figure 5). We have already described the projections onto specific levels of the TS; yet a full description requires modeling of the evolution from TS to final state. For this purpose we have carried out a second, separate set of calculations.

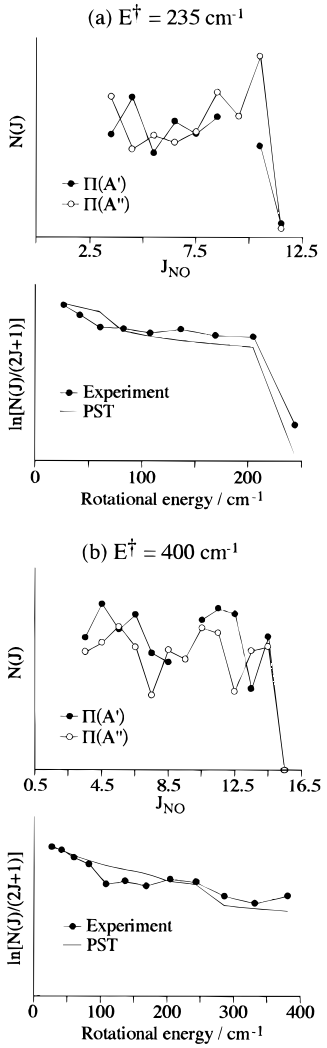

Figure 8. NO($^2\Pi_{1/2}$) rotational state distributions obtained at (a) $E^\dagger$ = 235 cm^{-1} and (b) $E^\dagger$ = 400 cm^{-1} following IR−visible excitation. The upper panel in each part displays the distributions in the two (A′,A″) Λ-doublet states of NO($^2\Pi_{1/2}$); the lower panels compare semilog plots of the distributions summed over Λ-doublet levels with PST. (Adapted from ref 22.)

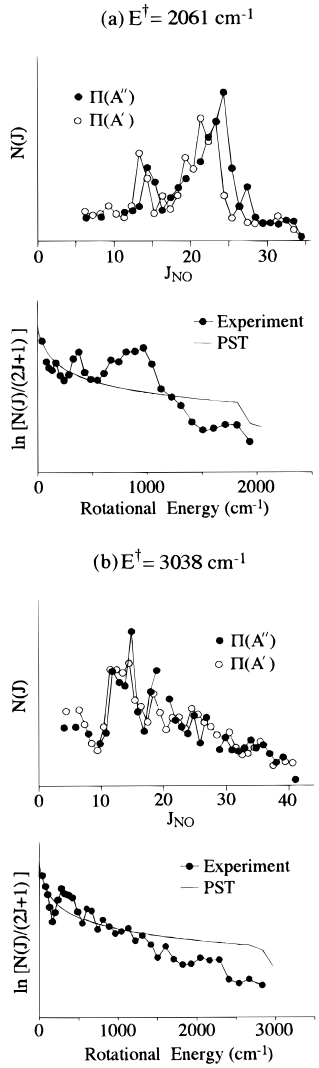

Figure 9. NO($^2\Pi_{1/2}$) rotational state distributions obtained at (a) $E^\dagger$ = 2061 cm^{-1} and (b) $E^\dagger$ = 3038 cm^{-1} following one-photon excitation. The format follows that of Figure 8. (Adapted from ref 21.)

In the modeling we have made several simplifying assumptions. First, we assume that every energetically available TS level has a statistical random population. Second, the passage from TS to final state is assumed to be much more rapid than that from Franck−Condon (i.e., equilibrium) regin to TS. Our last, and most severe, assumption is that the evolution of the bending-like TS wave functions into final states is sudden.

We express the TS wave function (Ψ) as a linear combination of harmonic oscillator TS basis functions whose complex coefficients are randomly weighted:

$$\Psi = \sum_n C_n e^{\phi_n} \Psi_n(\theta) \qquad (11)$$

where θ is the TS bending angle. As a limiting case for the evolution from TS to products, we use the Franck−Condon model for dissociation[73−75] and assume no exit-channel interactions beyond the TS. Using parameters appropriate for NO_2,[22,45,57] NO rotational state distributions were calculated by expanding the TS wave function into a basis set of spherical harmonics (i.e., NO free rotor) wave functions, and the raw distributions were smoothed to reduce fast oscillations shown to be unobservable under most experimental conditions.[75−77]

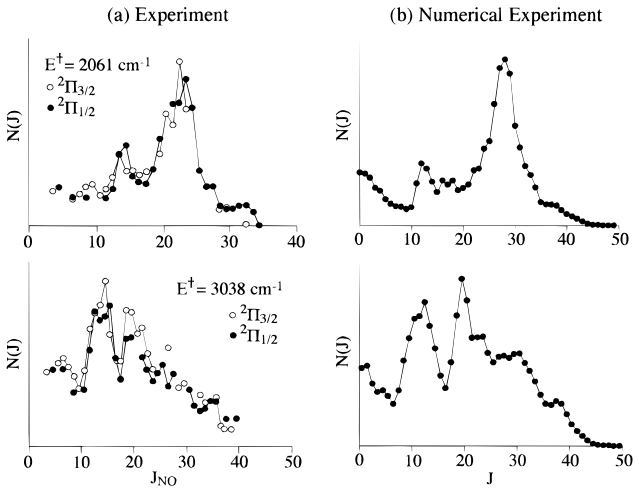

Figure 10. (a) NO($^2\Pi_{1/2}$) and ($^2\Pi_{3/2}$) rotational state distributions obtained at $E^\dagger$ = 2061 and 3038 cm^{-1} following one-photon excitation. (b) Calculated distributions using Franck−Condon mapping of harmonic TS basis functions whose complex coefficients are randomly weighted, as described in the text. (From ref 22.)

Displayed in Figure 10 are the results of two such calculations and two experimental one-photon NO distributions obtained at $E^\dagger$ = 2061 and 3038 cm^{-1}, respectively. Distributions in both

NO spin−orbit states are shown, each summed over Λ-doublet level. Although the similarity between calculated and experimental distributions is striking, we again emphasize that it is not our intent to *simulate* the experimental distributions. These calculated distributions were chosen from a large sample of random runs *because* of their remarkable similarity to experiment and thus their ability to demonstrate the main features of the experimental distributions (e.g., prominent oscillatory structures which vary for different random weightings of the TS levels).[19] It is noteworthy that in order to produce structured distributions which vary with different (random) weightings, *complex* coefficients (i.e., including phases) must be used to assure interference. A simple superposition of amplitudes (i.e., the use of real coefficients) does not reproduce the pronounced changes in oscillatory structures with $E^\dagger$. We note that Peskin *et al*. have shown that when their random matrix approach is combined with dynamical matrix elements representing the sudden approximation, a qualitatively similar behavior is obtained.[65] Thus, the simulated distributions for the tight TS show that the populations of adjacent rotational levels may be correlated in a way that reflects the superposition of the populated TS levels. Further discussion is provided in refs 65 and 78.

The overall success of this model in *qualitatively* reproducing our experimental observations is encouraging and supports our picture of NO_2 decomposition. Fluctuations are predicted in the NO rotational distributions at energies near threshold where the TS is loose. At higher energies, the onset of larger oscillatory structures is associated with the bending-like levels of tighter TS and the decrease in exit-channel energy transfer.[72] Despite its success, the validity of this model extends no farther than that of its assumptions, of which perhaps the most critical is that of no final state interaction beyond the TS. Although this assumption cannot be tested at present, it is plausible that with increasing $E^\dagger$, and thus more rapid dissociation, the sudden approximation used in this model becomes increasingly valid.

E. Fluctuations in the Electronic Degree of Freedom: Correlated Spin−Orbit Distributions. Thus far, we have documented the existence of marked fluctuations and oscillations in the nuclear degrees of freedom of the NO product. It is intriguing to see whether the electronic degrees of freedom will exhibit fluctuations as well. Accurately describing the spin−orbit distributions in unimolecular decomposition is important not only in understanding nonadiabatic transitions among electronic states but also for calculations of unimolecular reaction rates, where knowledge of the effective electronic state degeneracies is required. To this end measurements of spatial recoil profiles of specific $v = 0$; j, Ω, Λ states of NO were used to infer the relative populations of the atomic oxygen spin−orbit states correlated with single, specific quantum states of $NO(^2\Pi_\Omega;v{=}0;J;\Lambda)$.[23]

In this method, NO_2 is expanded in a molecular beam and photolyzed by a laser polarized in a direction perpendicular to the velocity vector of the molecular beam. The nearly parallel $1^2B_2 \leftarrow 1^2A_1$ transition leads to product recoil predominantly along the laser polarization axis. After a time delay, the products reach the detection region, which is separated spatially from the photolysis region. Due to their different recoil velocities, $NO(^2\Pi_\Omega,J,\Lambda)$ products correlated with different $O(^3P_j)$ spin−orbit states reach the detection region spatially separated. By scanning the position of the probe laser, the spatial profile of a state-selected NO product is obtained, and typical examples are shown in Figure 11. The correlation between the $NO(^2\Pi_\Omega,J,\Lambda)$ translational and internal energies

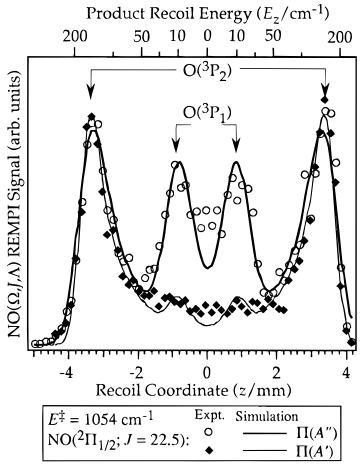

Figure 11. Spatial profiles of the two (A′,A″) Λ-doublet states of $NO(^2\Pi_{1/2},J{=}10.5)$ obtained at $E^\dagger = 1054$ cm^{-1} and their least-squares fits. The arrows indicate the peaks correlated with the $^3P_2$ and $^3P_1$ spin−orbit states of the O atom. Note the large difference in the $O(^3P_{1,2})$ relative populations in the two profiles. (From ref 23.)

is used to generate the relative populations of $O(^3P_{j=2,1,0})$ from the NO spatial recoil profiles.

The state-specific $O(^3P_j)$ population ratios show significant fluctuations with respect to the quantum state of the correlated $NO(^2\Pi_\Omega,J,\Lambda)$ fragment. Prominent fluctuations are observed: (i) at specific $E^\dagger$ when monitoring different NO rotational states or the two Λ-doublet components of the same rotational state (Figure 11) and (ii) when monitoring a specific NO state at slightly different $E^\dagger$. Thus, the state-to-state nonadiabatic transitions between surfaces correlating with different $O(^3P_j)$ + $NO(^2\Pi_\Omega)$ channels fluctuate in the same manner observed previously for the rotational states of NO in the same energy region. The fluctuations in the fully resolved $O(^3P_j)$ distributions do not appear to diminish with excess energy. On average, however, the $O(^3P_j)$ population ratios are much colder than statistical and, when summed over all studied NO channels, agree with the results of Miyawaki *et al*.[52] Moreover, the $O(^3P_1)$:$O(^3P_2)$ population ratios correlated with $NO(^2\Pi_{3/2})$ are on average larger than those correlated with the ground spin−orbit state, $NO(^2\Pi_{1/2})$. This is in accordance with recent calculations of Katagiri and Kato (see section III.A.3).[57]

F. Fluctuations in State-to-State Rates? Alignment Measurements of the NO Fragment. The decomposition rates [$k(E)$] of jet-cooled NO_2 are in fair agreement with the predictions of statistical theories.[26g,43−45] However, due to the short NO_2 decomposition lifetimes (i.e., less than a few picoseconds), the time-resolved measurements are necessarily averaged over many initial levels and summed over many product channels and therefore cannot exhibit state-to-state fluctuations. Fluctuations of rates about the RRKM average have been observed in other systems (e.g., H_2CO, CH_3O)[79,80] near threshold or in the tunneling regime. In these cases the resonances are mostly isolated, and therefore their widths are related to the decay rates as per eq 3. Since in NO_2 the widths of the spectral features cannot be converted directly to rates,[72] (but see ref 65 for an indirect way) and time-resolved measurements yield only averaged values, we have searched for fluctuations using an indirect measure of the decomposition rates; namely, in the rotational alignment of the NO fragment.

The alignment parameter $\mathbf{A}_0^{(2)}$ characterizes the correlation between the electronic transition moment $\boldsymbol{\mu}$ in the parent and the fragment angular momentum $\mathbf{J}$.[81,82] The limiting cases of $\mathbf{J}\|\boldsymbol{\mu}$ and $\mathbf{J}\perp\boldsymbol{\mu}$ correspond to $\mathbf{A}_0^{(2)} = 0.8$ and -0.4, respectively. For the NO_2 $^2B_2 \leftarrow {}^2A_1$ transition, $\boldsymbol{\mu}$ lies in the molecular plane;

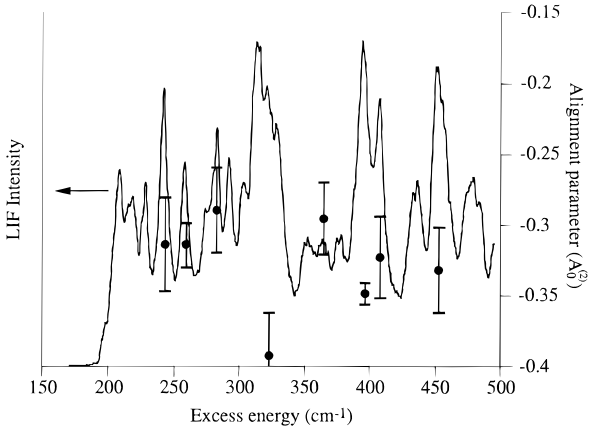

Figure 12. One-photon PHOFRY spectrum (solid line) and measured $A_0^{(2)}$ values (filled circles) in the range $E^\dagger = 150-500$ cm^{-1} obtained for NO($^2\Pi_{1/2}$,v=0,J=10.5). The $A_0^{(2)}$ values are corrected for hyperfine depolarization as described in the text; error bars represent $\pm 1\sigma$.

$\mathbf{A}_0^{(2)} = -0.4$ is therefore expected if dissociation occurs much faster than parent rotation, but this value increases at higher rotational temperatures or when the dissociation is slow.[55,72,83]

To determine $\mathbf{A}_0^{(2)}$ for a given NO quantum state, we measure the LIF intensity for different photolysis-probe geometries (I and II as denoted by Dixon).[84] This is accomplished by 90° rotation of the photolysis laser polarization on alternate laser shots using a photoelastic modulator. At each photolysis wavelength typically 10^5 laser shots were averaged at each polarization. Figure 12 displays both a series of alignment measurements and a one-photon PHOFRY spectrum at $E^\dagger = 150-500$ cm^{-1} obtained by monitoring the $Q_{11}(10.5)$ transition of NO($^2\Pi_{1/2}$,v=0). Error bars for the alignment measurements represent $\pm 1\sigma$. The measured $\mathbf{A}_0^{(2)}$ values fluctuate as a function of $E^\dagger$, and similar behavior is obtained when monitoring different rotational levels.[72] To correct for hyperfine depolarization,[81] we measured $\mathbf{A}_0^{(2)}$ for both $Q_{11}(10.5)$ and $Q_{11}(20.5)$ at higher $E^\dagger$ and normalized to these values, assuming depolarization was insignificant at $J \geq 20.5$.[54] After correction, the average alignment ranges from ~ -0.3 at $E^\dagger = 250$ cm^{-1} to ~ -0.35 at $E^\dagger > 400$ cm^{-1}. Similar values were reported by Miyawaki *et al.* in this energy region.[29]

Since fluctuations are found in virtually every observable concerning NO_2 decomposition (e.g., PSD's, PHOFRY spectra) and fluctuations in width have been observed in the case of isolated resonances,[79,80,85−88] it is not surprising to observe fluctuations in $\mathbf{A}_0^{(2)}$. However, caution should be exercised in interpreting these results. The fluctuations could indeed reflect lifetime variances, i.e., state-to-state fluctuations in the rate, but other sources cannot be conclusively ruled out at this time.[72] Also, the average NO_2 decomposition lifetimes are fast enough even at these modest energies to render the average alignment near its maximum value, making observation of the full extent of the fluctuations difficult (i.e., only lifetimes longer than the average will be observed). More work is clearly needed to confirm the existence of state-to-state fluctuations in $k(E)$. We note that the recoil anisotropy parameter, β, has also been shown to depend on the quantum state of NO.[41b,89]

III. NO Product State Distributions: Comparisons with Statistical Theories and Implications for the TS

In this section we compare the product state distributions with predictions of statistical models and discuss the implications of our findings to the TS. Studies of the decompositions of NCNO[8,90] and CH_2CO[9,91,92] have shown good agreement with PST for diatomic fragment rotational distributions and with SSE/PST and variational RRKM theory for fragment vibrations. The agreement between experiment and theory in these cases indicates that the basic assumptions of these theories are justified even in such fast dissociating small molecules. However, in these molecules each quantum state of one fragment is typically correlated with many states of the other, so averaging is inherent. In this regard, NO_2 decomposition provides further tests for the validity of statistical treatments regarding PSD's. Details of the models used to calculate the statistical distributions can be found in several excellent monographs and review articles[6,8,9,24−26] and therefore will not be elaborated upon here.

A. Product State Distributions. *A.1. NO Rotational and Vibrational Distributions.* Figures 8 and 9 display selected NO rotational distributions from decomposition of jet-cooled NO_2 obtained following both one-photon and IR−visible excitation. As discussed in section II, at excess energies near threshold (i.e., $E^\dagger = 0-400$ cm^{-1}) apparently random fluctuations are seen in the *individual* Λ-doublet level distributions of the NO(v=0) fragment. However, these fluctuations consistently scatter about the theoretical predictions of PST as seen in Figure 8. Distributions obtained by summing over Λ-doublet levels show reduced fluctuations and good agreement with theory, even for IR−visible excitation. It is clear that NO rotational distributions at these energies are in qualitative agreement with PST expectations. We note that similar behavior is observed in NO(v=1) distributions at excess energies near the $v = 1$ threshold.[19,72]

The representative NO(v=0) rotational distributions shown in Figure 9 for higher excess energies (e.g., $E^\dagger > 2000$ cm^{-1}) display pronounced oscillatory structures which are well reproduced in the two Λ-doublet level distributions and are not diminished when summing over Λ-doublet level. We have shown in section II that these oscillations can be modeled qualitatively by mapping bending-like wave functions associated with a *tight* TS into free rotor states of the NO fragment. Why, then, do these oscillations consistently cluster about the statistical predictions of PST, which assumes a very loose TS? This can be reconciled by recognizing that the range of rotational excitations allowed in Franck−Condon mapping is a sensitive function of the TS bending angle and frequency. The TS parameters used in the calculations presented in section II, which are based on values derived from ab initio calculations,[45,57] happen to correspond to rotational excitations that cover the full range allowed by energy conservation at all energies studied ($E^\dagger < 3038$ cm^{-1}). The qualitative agreement observed with PST at these energies thus reflects in part the specific geometry of the tight TS and does not constitute a valid test for the looseness of the TS. This is an important recurrent theme; distributions which can be fit by a statistical model do not prove that such a model correctly describes the dissociation mechanism. The observation of PST-like distributions even when the TS has tightened may also arise from exit-channel interactions beyond the TS, which can lead to population of all levels allowed by energy and angular momentum conservation. This effect is probably more important at lower energies, where recoil velocities are small.[19,72] The relative populations of NO(v=1) measured by us at a number of excess energies, from the energetic threshold of NO(v=1) at $E^\dagger = 1876-3038$ cm^{-1}, are shown in Figure 13 along with the predictions of variational RRKM theory.[45] Good qualitative agreement is observed, although the experimental values tend to fluctuate about the statistical predictions. We note that rather statistical vibrational state distributions persist at least up to $E^\dagger = 7222$ cm^{-1}.[60,61]

A.2. Spin−Orbit State Distributions. We have seen that NO rotational and vibrational state distributions from NO_2 decom-

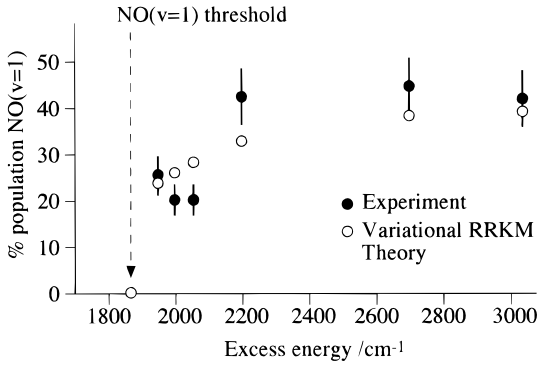

Figure 13. Measured and calculated NO(v=1) relative populations as a function of excess energy from the NO(v=1) threshold at $E^{\dagger} = 1876-3038$ cm^{-1}. The calculated distribution was obtained from the variational RRKM calculations of ref 45. (Adapted from ref 19b).

position at $E^{\dagger} = 0-3038$ cm^{-1} can be described within the framework of statistical theories. In contrast, the NO($^2\Pi_\Omega$;Ω= 1/2,3/2) spin−orbit state distributions over the same range are colder than predicted by statistical models, in both the $v = 0$ and $v = 1$ channels.[19] Similarly, colder than statistical spin−orbit state distributions are found for the O(^3P_j;j=2,1,0) fragment.[23,52] While the relative O(^3P_j) populations show marked fluctuations with excess energy,[23,52] the overall ratio NO($^2\Pi_{1/2}$;v=0,1)/NO($^2\Pi_{3/2}$;v=0,1) ∼ 3 varies only slightly with photolysis energy over this range.[19]

To explain the experimental spin−orbit state distributions, we refer to recent work of Katagiri and Kato,[57] who calculated all 18 doubly degenerate O−NO PESs correlated with the various NO($^2\Pi_\Omega$) + O(^3P_j) asymptotes. Using these potentials and a simplified dissociation model, average spin−orbit state distributions of both fragments were calculated, in good agreement with experiment. Of the 18 surfaces, only two are attractive, both correlating with the NO($^2\Pi_{1/2}$) + O($^3P_2$) asymptote. Calculations show that the splitting between attractive and repulsive surfaces increases at smaller O−NO separation, suggesting a decreasing probability for nonadiabatic transitions between these surfaces at smaller separations. Since only the lowest attractive surfaces correlate with the ground electronic state of NO_2 on which the reaction occurs, the observation of cold spin−orbit state distributions in both fragments is not surprising. These calculations also predict the trends in correlated NO($^2\Pi_\Omega$) + O(^3P_j) distributions described in section II.E.

B. Implications for the Transition State. As discussed above, the TS in unimolecular reactions is well-defined when it relates to rates; however, the PSD's can be further modified beyond the TS via exit-channel interactions. In the case of distinct exit-channel barriers, dynamical signatures are usually prominent, as in other fast photodissociation processes. In the absence of such barriers, the exit-channel gradients are typically small and recoil velocities are low, especially for products whose internal energies approach $E^{\dagger}$. As a consequence, the dynamics in this case is rarely dominated by simple propensity rules. Energy exchange beyond the TS is governed by a subtle interplay between the size of the energy quantum to be transferred and the relative recoil velocity.

NO vibrations (∼1800 cm^{-1}) exchange energy inefficiently and are thought to evolve adiabatically.[21,22,45] It appears that, for each NO vibration, the TS is loose near its appearance threshold and tightens progressively as $E^{\dagger}$ increases.[21,29,44,45] This is also revealed by the change in fluctuation patterns in the NO rotational state distributions.[21,22,72] For both $v = 0$ and $v = 1$, the fluctuations change from random to more regular oscillatory structures as $E^{\dagger}$ increases, reflecting the tightening of the TS. When the TS tightens and its levels become bending-like, agreement with PST may signify either efficient exit-channel interactions beyond the TS or mappings of wave functions of a TS whose geometry happens to produce PST-like distributions. In the case of NO_2, it is possible that both factors contribute to the average PST-like appearance of the rotational distributions, while the appearance of prominent oscillations whose shapes depend sensitively on $E^{\dagger}$ are the prime indicators of the tightening of the TS.

The similarity of oscillatory patterns obtained in the rotational distributions of the two spin−orbit states of NO has led us to suggest that the spin−orbit distributions are fixed last, at long range, where the potential curves correlating with different spin−orbit pairs are close.[21] Recent ab-initio calculations confirm this interpretation.[57] Thus, the PSD's in NO_2 decomposition indicate that a hierarchy of adiabaticity exists. NO vibrations are fixed first, at the shortest O−NO separations, followed by the rotational distributions with their typical oscillatory patterns at higher $E^{\dagger}$. The different electronic channels correlated with the different spin−orbit states of NO and O are determined only at large internuclear separations.

IV. Concluding Remarks

In this article, we present the unimolecular reaction of NO_2 from the perspective of resonance scattering, while interpretations are couched in terms of statistical theories. The concepts used in the interpretations have been developed for several decades, and their implementation and refinement awaited only the advent of state-resolved experimental techniques. That statistical theories do well in describing, on the average, the decomposition of a molecule as small as NO_2 is a tribute to the power of the statistical approach in describing processes that involve deep attractive wells. It is also remarkable that even a limited incoherent superposition of initial states (such as in a 5 K molecular beam) is sufficient to partially wash out interference effects. At higher temperatures, NO_2 exhibits the smooth, statistical behavior observed in larger molecules. Thus, when the density of states is small and the initial and final states are well-defined, deviations from statistical expectations first manifest themselves in the form of fluctuations and oscillations. Removal of incoherent averaging by state selection enabled us to explore the experimental manifestations of overlapping resonances and the various sources of fluctuations.

From the perspective of statistical theories, state-to-state studies enable the testing of underlying assumptions of the models and have led to rapid advances in the detailed understanding of simple bond-fission reactions. In particular, the studies described here show that the definition of a TS, while clear when applied to decomposition rates, is not a simple one with regard to PSD's. It may be more useful to speak in terms of regions along the reaction coordinate where the various degrees of freedom become adiabatic. This, in turn, will depend on $E^{\dagger}$ and thus on final state interactions.

Our studies have shown that in the decomposition of NO_2 a hierarchy of adiabaticity exists, with vibrations becoming adiabatic first and spin−orbit distributions last. In triatomic molecules, the patterns of fluctuations and oscillations enable us to gain insight into regions of the PES near and beyond the TS. In larger molecules, studies of *correlated* distributions and vector properties should be likewise useful,[23,93,94] and additional studies are currently underway.[95,96] We also conclude that agreement between the rotational distributions and PST is not a good test for the looseness of the TS. In certain circumstances (e.g., specific geometries of the TS, existence of exit-channel interactions), a tight TS will give rise to rotational distributions

similar to those predicted by PST, even though the latter assumes a very loose, fragmentlike TS. In NO_2, the experimental indication that the TS has tightened comes from the change of fluctuation patterns in the rotational distributions.

We point out that the concept of a TS is not needed when full quantum scattering calculations on realistic PES's are feasible. Such calculations can, in principle, describe the evolution of the system from reactants to products in terms of scattering matrix elements, but are still exceedingly difficult for decomposition of molecules with deep potential wells. Nevertheless, impressive progress has been made recently, and calculations of overlapping resonances and unimolecular reactions of small molecules (e.g., HOCO, HO_2)[97,98] have begun to appear, showing both the existence of overlapping resonances and fluctuations and the connection with RRKM theory. Even the elusive problem of spin−orbit populations in statistical decompositions has recently been tackled in the framework of restricted ab-initio calculations.[57] With the continuing development of more efficient computational techniques, many of the conclusions reached by the random matrix formulation of the optical model and its simple version presented here will be tested and refined for realistic systems.

Since manifestations of interferences among overlapping resonances have been identified experimentally only in the unimolecular decompositions of NO_2 and H_2CO,[9,99] it is important to ask how general this phenomenon is and under what conditions it is best observed. Two points are relevant here. First, fluctuations in rotational distributions have been observed also in dissociation from isolated resonances (e.g., HCO),[87] as well as in direct photodissociation from well-defined parent initial states (e.g., H_2O).[100] Overlapping resonances are implicated only when the partial spectra show variations in shapes, widths, and intensities of the observed features as a function of the monitored fragment state or in other cases where strongly asymmetric line shapes are observed.[99,101] Second, we believe that fluctuations and oscillations due to overlapping resonances will be observed in other simple bond fission reactions of small molecules when the initial state is well-defined and one of the products is an atom. Monitoring specific quantum states of the associated polyatomic fragment should reveal the signatures of overlapping resonances, when the overlap parameter is significant, but the number of independent decay channels is not too large.

Despite the fast recent progress in our understanding of unimolecular reactions, there are clearly areas that require further investigation. Examples include the role of parent rotation and centrifugal barriers (e.g., measurements of $k(E,J)$,[102] the roles of long-range forces and exit-channel interactions, the issue of adiabatic evolution of the different degrees of freedom, the manifestations of restricted IVR and its dependence on $E^{\dagger}$, and the transition from statistics to dynamics at high $E^{\dagger}$.[61] The continued interplay between experiment and theory will continue to challenge us for years to come, finally revealing the full richness of simple bond-fission reactions.

Acknowledgment. First and foremost we thank our collaborators in the studies of NO_2 decomposition, Martin Hunter, Jennifer Merlic-Bates, Dan Robie, Andrei Sanov, Craig Bieler, Uri Peskin, and Bill Miller, whose enthusiasm, perseverance, insight, and hard labors have made the work described here possible. We benefited greatly from discussions with Curt Wittig, C. Bradley Moore, Jürgen Troe, Stephen Klippenstein, Reinhard Schinke, and Howard Taylor. We thank Dr. Kaoru Yamanouchi for sending us the results presented in Figure 2a and Andrei Sanov for the careful reading of the manuscript. The U.S. National Science Foundation, Army Research Office, and Department of Energy supported various aspects of the research described here.

References and Notes

(1) Forst, W. *Theory of Unimolecular Reactions*; Academic: New York, 1973.
(2) Robinson, P. J.; Holbrook, K. A. *Unimolecular Reactions*; Wiley: New York, 1972.
(3) Benson, S. W. *Thermochemical Kinetics*, 2nd ed.; Wiley: New York, 1976.
(4) Gilbert, R. G.; Smith, S. C. *Theory of Unimolecular and Recombination Reactions*; Blackwell: Oxford, 1990.
(5) Pritchard, H. O. *The Quantum Theory of Unimolecular Reactions*; Cambridge University Press: Cambridge, 1984.
(6) Baer, T.; Hase, W. L. *Unimolecular Reaction Dynamics*: *Theory and Experiments*; Oxford University Press: Oxford, in press.
(7) Crim, F. F. *Annu. Rev. Phys. Chem.* **1984**, *35*, 657.
(8) (a) Reisler, H.; Wittig, C. *Annu. Rev. Phys. Chem.* **1986**, *37*, 307. (b) Reisler, H.; Wittig, C. In *Advances in Kinetics and Dynamics*; Barker, J. R., Ed.; JAI Press: Greenwich, 1992; Vol. 1.
(9) Greene, Jr., W. H.; Moore, C. B.; Polik, W. F. *Annu. Rev. Phys. Chem.* **1992**, *43*, 307.
(10) Blatt, J. M.; Weisskopf, V. F. *Theoretical Nuclear Physics*; Wiley: New York, 1952.
(11) Bohr, N. *Nature* **1936**, *137*, 344.
(12) Feshbach, H. *Theoretical Nuclear Physics*; Wiley: New York, 1992.
(13) Levine, R. D. *Quantum Mechanics of Molecular Rate Processes*; Clarendon: Oxford, 1969.
(14) (a) Ericson, T. *Ann. Phys.* **1963**, *23*, 390; (b) *Phys. Rev. Lett.* **1960**, *5*, 430.
(15) Hodgson, P. E. *Nuclear Reactions and Nuclear Structure*; Clarendon: Oxford, 1971.
(16) Shaw, R. W.; Norman, J. C.; Vandenbosch, R.; Bishop, C. J. *Phys. Rev.* **1969**, *184*, 1040.
(17) Mies, F. H.; Krauss, M. *J. Chem. Phys.* **1966**, *45*, 4455.
(18) Mies, F. H. *Phys. Rev.* **1968**, *175*, 164.
(19) (a) Robie, D. C.; Hunter, M.; Bates, J. L.; Reisler, H. *Chem. Phys. Lett.* **1992**, *192*, 279. (b) Hunter, M.; Reid, S. A.; Robie, D. C.; Reisler, H. *J. Chem. Phys.* **1993**, *99*, 1093.
(20) Reid, S. A.; Brandon, J. T.; Hunter, M.; Reisler, H. *J. Chem. Phys.* **1993**, *99*, 4860.
(21) Reid, S. A.; Robie, D. C.; Reisler, H. *J. Chem. Phys.* **1994**, *100*, 4256.
(22) Reid, S. A.; Reisler, H. *J. Chem. Phys.* **1994**, *101*, 5683.
(23) Sanov, A.; Bieler, C. R.; Reisler, H. *J. Phys. Chem.* **1995**, *99*, 13637.
(24) (a) Wardlaw, D. M.; Marcus, R. A. *Adv. Chem. Phys.* **1988**, *70*, 231. (b) Marcus, R. *Philos. Trans. R. Soc. London, Ser. A* **1990**, *332*, 283 and references therein.
(25) (a) Pechukas, P.; Light, J. C.; Rankin, C. *J. Chem. Phys.* **1966**, *44*, 794. (b) Pechukas, P.; Light, J. C. *Ibid.* **1965**, *42*, 3281. (c) Light, J. C. *Discuss. Faraday Soc.* **1967**, *44*, 14.
(26) (a) Quack, M.; Troe, J. *Ber. Bunsen-Ges. Phys. Chem.* **1974**, *78*, 240. (b) **1974**, *79*, 171. (c) **1975**, *79*, 469. (d) **1977**, *81*, 329. (e) Troe, J. *J. Chem. Phys.* **1977**, *66*, 4758. (f) **1981**, *75*, 2261. (g) **1983**, *79*, 60. (h) *J. Phys. Chem.* **1979**, *83*, 114.
(27) Fano, U. *Phys. Rev.* **1961**, *124*, 1866.
(28) (a) Robra, U.; Zacharias, H.; Welge, K. H. *Z. Phys. D.* **1990**, *16*, 175. (b) Robra, U. Ph.D. Thesis, University of Bielefeld, 1984.
(29) Miyawaki, J.; Yamanouchi, K.; Tsuchiya, S. *J. Chem. Phys.* **1993**, *99*, 254.
(30) Ionov, S. I.; Davis, H. F.; Mikhaylichenko, K.; Valachovic, L.; Beaudet, R. A.; Wittig, C. *J. Chem. Phys.* **1994**, *101*, 4809.
(31) Miyawaki, J.; Yamanouchi, K.; Tsuchiya, S. *J. Chem. Phys.* **1994**, *101*, 4505.
(32) (a) Douglas, A. E.; Huber, K. P. *Can. J. Phys.* **1965**, *43*, 74. (b) Douglas, A. E. *J. Chem. Phys.* **1966**, *45*, 1007.
(33) (a) Hsu, D.; Monts, D. L.; Zare, R. N. *Spectral Atlas of Nitrogen Dioxide 5530 to 6480 Å*; Academic: New York, 1978. (b) Brucat, P. J.; Zare, R. N. *Mol. Phys.* **1985**, *55*, 277.
(34) (a) Köppel, H.; Domcke, W.; Cederbaum, L. S. *Adv. Chem. Phys.* **1984**, *57*, 59. (b) Haller, E.; Köppel, H.; Cederbaum, L. S. *J. Mol. Spectrosc.* **1985**, *111*, 377. (c) Zimmermann, Th.; Köppel, H.; Cederbaum, L. S. *J. Chem. Phys.* **1989**, *91*, 3934. (d) Zimmermann, Th.; Cederbaum, L. S.; Meyer, H.-D.; Köppel, H. *J. Phys. Chem.* **1987**, *91*, 4446. (e) Zimmermann, Th.; Cederbaum, L. S.; Köppel, H. *Ber. Bunsen-Ges. Phys. Chem.* **1988**, *92*, 217.
(35) Brand, J. C. D.; Chiu, P. H. *J. Mol. Spectrosc.* **1977**, *75*, 1.
(36) (a) Persch, G.; Vedder, H. J.; Demtröder, W. *Chem. Phys.* **1986**, *105*, 471. (b) *J. Mol. Spectrosc.* **1987**, *123*, 356. (c) Vedder, H. J.; Schwarz, M.; Foth, H.-J.; Demtröder, W. *Ibid.* **1983**, *97*, 92. (d) Persch, G.; Mehdizadeh, E.; Demtröder, W.; Zimmermann, Th.; Köppel, H.; Cederbaum, L. S. *Ber. Bunsen-Ges. Phys. Chem.* **1988**, *92*, 312.

(37) (a) Lehmann, K. K.; Coy, S. L. *J. Chem. Phys.* **1985**, *83*, 3290. (b) Coy, S. L.; Lehmann, K. K.; DeLucia, F. C. *Ibid.* **1986**, *85*, 4297. (c) Lehmann, K. K.; Coy, S. L. *Ber. Bunsen-Ges. Phys. Chem.* **1988**, *92*, 306.
(38) Hardwick, J. L. *J. Mol. Spectrosc.* **1985**, *109*, 85.
(39) Smalley, R. E.; Wharton, L.; Levy, D. H. *J. Chem. Phys.* **1975**, *63*, 4989.
(40) (a) Delon, A.; Jost, R. *J. Chem. Phys.* **1991**, *95*, 5686. (b) **1991**, *95*, 5700. (c) Georges, R.; Delon, A.; Jost, R. *J. Chem. Phys.* **1995**, *103*, 1732.
(41) (a) Butenhoff, T. J.; Rohlfing, E. A. *J. Chem. Phys.* **1993**, *99*, 5460. (b) **1993**, *99*, 5469.
(42) Chen, C. H.; Clark, D. W.; Payne, M. G.; Kramer, S. D. *Opt. Commun.* **1980**, *32*, 391.
(43) (a) Gaedtke, H.; Troe, J. *Ber. Bunsen-Ges. Phys. Chem.* **1975**, *79*, 184. (b) Quack, M.; Troe, J. *Ibid.* **1975**, *79*, 469. (c) Gaedtke, H.; Hippler, H.; Troe, J. *Chem. Phys. Lett.* **1972**, *16*, 177.
(44) (a) Brucker, G. A.; Ionov, S. I.; Chen, Y.; Wittig, C. *Chem. Phys. Lett.* **1992**, *194*, 301. (b) Ionov, S. I.; Brucker, G. A.; Jaques, C.; Chen, Y.; Wittig, C. *J. Chem. Phys.* **1993**, *99*, 3420. (c) Wittig, C.; Ionov, S. I. *J. Chem. Phys.* **1994**, *100*, 4717.
(45) Klippenstein, S. J.; Radivoyevitch, T. *J. Chem. Phys.* **1993**, *99*, 3644.
(46) Klippenstein, S. J. In *Advances in Physical Chemistry: The Chemical Dynamics and Kinetics of Small Radicals*; Liu, K., Wagner, A. F., Eds.; World Scientific: in press, 1995, and references therein.
(47) (a) Zacharias, H.; Geilhaupt, M.; Meier, K.; Welge, K. H. *J. Chem. Phys.* **1981**, *74*, 218. (b) Zacharias, H.; Meier, K.; Welge, K. H. In *Energy Storage and Redistribution in Molecules*; Hinze, J., Ed.; Plenum: New York, 1983.
(48) (a) Mons, M.; Dimicoli, I. *Chem. Phys. Lett.* **1986**, *131*, 298; (b) Chem. *Phys.* **1989**, *130*, 307.
(49) Kawasaki, M.; Sato, H.; Fukuroda, A.; Kikuchi, T.; Kobayashi, S.; Arikawa, T. *J. Chem. Phys.* **1987**, *86*, 4431.
(50) Chen, K.; Pei, C. *Chem. Phys. Lett.* **1987**, *137*, 361.
(51) Rubahn, H.-G.; van der Zande, W. J.; Zhang, R.; Bronikowski, M. J.; Zare, R. N. *Chem. Phys. Lett.* **1991**, *186*, 154.
(52) (a) Miyawaki, J.; Tsuchizawa, T.; Yamanouchi, K.; Tsuchiya, S. *Chem. Phys. Lett.* **1990**, *165*, 168. (b) Yamanouchi, K.; Takeuchi, S.; Tsuchiya, S. *J. Chem. Phys.* **1990**, *92*, 4044. (c) Miyawaki, J.; Yamanouchi, K.; Tsuchiya, S. *Chem. Phys. Lett.* **1991**, *180*, 287.
(53) Elofson, P.-A.; Ljungstrom, E. *J. Chem. Phys.* **1992**, *165*, 323.
(54) Changalong, N.; Hua, L.; Pfab, J. *J. Phys. Chem.* **1993**, *97*, 7458.
(55) Hradil, V. P.; Suzuki, T.; Hewitt, S. A.; Houston, P. L.; Whitaker, B. J. *J. Chem. Phys.* **1993**, *99*, 4455.
(56) Rohlfing, E. A.; Valentini, J. J. *J. Chem. Phys.* **1985**, *83*, 521.
(57) Katagiri, H.; Kato, S. *J. Chem. Phys.* **1993**, *99*, 8805.
(58) Busch, G. E.; Wilson, K. *J. Chem. Phys.* **1972**, *56*, 3626, 3638.
(59) McFarlane, J.; Polanyi, J. C.; Shapter, J. G. *J. Photochem. Photobiol. A: Chem.* **1991**, *58*, 139.
(60) Harrison, J. A.; Yang, X.; Rösslein, M.; Felder, P.; Huber, J. R. *J. Phys. Chem.* **1994**, *98*, 12260.
(61) Knepp, P. T.; Terentis, A. C.; Kable, S. H. *J. Chem. Phys.* **1995**, *103*, 194.
(62) Levy, D. H.; Wharton, L.; Smalley, R. E. In *Chemical and Biochemical Applications of Lasers*; Academic: New York, 1977; Vol. 2.
(63) Rotter, I. *Rep. Prog. Phys.* **1991**, *54*, 635.
(64) Peskin, U.; Reisler, H.; Miller, W. H. *J. Chem. Phys.* **1994**, *101*, 9672.
(65) Peskin, U.; Miller, W. H.; Reisler, H. *J. Chem. Phys.* **1995**, *102*, 8874.
(66) Levine, R. D. *Ber. Bunsen-Ges. Phys. Chem.* **1988**, *92*, 222.
(67) (a) Miller, W. H.; Hernandez, R.; Moore, C. B.; Polik, W. F. *J. Chem. Phys.* **1990**, *93*, 5657. (b) Hernandez, R.; Miller, W. H.; Moore, C. B.; Polik, W. F. *Ibid.* **1993**, *99*, 950.
(68) For isolated resonances a_m is proportional to $\Gamma_m/2\pi$; however, for overlapping resonances it is not rigorously clear what the correct normalization is. The effect of normalization by Γ_m is small when the number of effective channels is large and the width of the Γ_m distribution is small.
(69) (a) Press, W. H.; Teukolsky, S. A.; Vettering, W. T.; Flannery, B. R. *Numerical Recipes in Fortran: The Art of Scientific Computing*; Cambridge University Press: Cambridge, 1992. (b) Dagpunar, J. *Principles of Random Variate Generation*; Oxford University Press: Oxford, 1988.
(70) Tramer, A.; Voltz, R. In *Excited States*; Academic: New York, 1979; Vol. 4.
(71) Delon, A.; Dupre, P.; Jost, R. *J. Chem. Phys.* **1993**, *99*, 9482.
(72) Reid, S. A.; Sanov, A.; Reisler, H. *R. Soc. Faraday Discuss.*, in press.
(73) (a) Morse, M. D.; Freed, K. F. *J. Chem. Phys.* **1981**, *74*, 4395; **1983**, *78*, 6045. (b) Morse, M. D.; Freed, K. F.; Band, Y. B. *J. Chem. Phys.* **1979**, *70*, 3064, 3620. (c) Freed, K. F.; Band, Y. B. In *Excited States*; Lim, E., Ed.; Academic: New York, 1978; Vol. 3.
(74) Beswick, J. A.; Gelbart, W. M. *J. Phys. Chem.* **1980**, *84*, 3148.
(75) Qian, C. X. W.; Ogai, A.; Brandon, J.; Bai, Y. Y.; Reisler, H. *J. Phys. Chem.* **1991**, *95*, 6763.
(76) Grinberg, H.; Freed, K. F.; Williams, C. J. *J. Chem. Phys.* **1990**, *92*, 7283.
(77) Schinke, R.; Engel, V.; Staemmler, V. *J. Chem. Phys.* **1985**, *83*, 4522.
(78) Reisler, H.; Keller, H.-M.; Schinke, R. *Comments At. Mol. Phys.* **1994**, *30*, 191.
(79) (a) Polik, W. F.; Guyer, D. R.; Moore, C. B. *J. Chem. Phys.* **1990**, *92*, 3453. (b) Polik, W. F.; Guyer, D. R.; Miller, W. H.; Moore, C. B. *Ibid.* **1990**, *92*, 3471.
(80) Geers, A.; Kappert, J.; Temps, F.; Weibrecht, J. W. *J. Chem. Phys.* **1990**, *93*, 1472; **1993**, *99*, 2271; **1994**, *101*, 3618; **1994**, *101*, 3634.
(81) (a) Green, C. H.; Zare, R. N. *Annu. Rev. Phys. Chem.* **1982**, *33*, 119. (b) Green, C. H.; Zare, R. N. *J. Chem. Phys.* **1983**, *78*, 6741.
(82) Fano, U.; Macek, J. H. *Rev. Mod. Phys.* **1973**, *45*, 553.
(83) Jonah, C. *J. Chem. Phys.* **1971**, *55*, 1915.
(84) Dixon, R. N. *J. Chem. Phys.* **1986**, *85*, 1866.
(85) Adamson, G. W.; Zhao, Z.; Field, R. W. *J. Mol. Spectrosc.* **1993**, *160*, 11.
(86) Neyer, D. W.; Luo, X.; Burak, I.; Houston, P. *J. Chem. Phys.* **1995**, *102*, 1645.
(87) Williams, S.; Tobiason, J. D.; Dunlop, J. R.; Rohlfing, E. A. *J. Chem. Phys.* **1995**, *102*, 8342.
(88) Tobiason, J. D.; Dunlop, J. R.; Rohlfing, E. A. *J. Chem. Phys.* **1995**, *103*, 1448.
(89) Meyer, H. Private communication, 1995.
(90) (a) Qian, C. X. W.; Noble, M.; Nadler, I.; Reisler, H.; Wittig, C. *J. Chem. Phys.* **1985**, *83*, 5573. (b) Wittig, C.; Nadler, I.; Reisler, H.; Noble, M.; Catanzarite, J.; Radhakrishnan, G. *Ibid.* **1985**, *83*, 5581.
(91) Garciamoreno, I.; Lovejoy, E. R.; Moore, C. B. *J. Chem. Phys.* **1994**, *100*, 8902.
(92) (a) Green, W. H.; Chen, I.-C.; Moore, C. B. *Ber. Bunsen-Ges. Phys. Chem.* **1988**, *92*, 389. (b) Chen, I.-C.; Green, W. H.; Moore, C. B. *J. Chem. Phys.* **1988**, *89*, 314.
(93) Qian, C. X. W.; Ogai, A.; Reisler, H.; Wittig, C. *J. Chem. Phys.* **1989**, *90*, 209.
(94) (a) Butenhoff, T. J.; Carleton, K.; Moore, C. B. *J. Chem. Phys.* **1990**, *92*, 377. (b) Carleton, K.; Butenhoff, T. J.; Moore, C. B. *Ibid.* **1990**, *93*, 3907. (c) Butenhoff, T. J.; Carleton, K.; Chuang, M.-C.; Moore, C. B. *J. Chem. Soc., Faraday Trans. 2* **1989**, *85*, 1155.
(95) Klippenstein, S. J.; Kline, J. *J. Chem. Phys.*, submitted.
(96) Drabbels, M.; Morgan, C. G.; McGuire, D. S.; Wodtke, A. M. *J. Chem. Phys.* **1995**, *102*, 611.
(97) (a) Hernandez, M.; Clary, D. C. *J. Chem. Phys.* **1994**, *101*, 2779. (b) Goldfield, E. M.; Gray, S. K.; Schalz, G. C. *J. Chem. Phys.* **1995**, *102*, 8807. (c) Zhang, D. H.; Zhang, J. Z. H. *J. Chem. Phys.* **1994**, *101*, 3671.
(98) Dobbyn, A. J.; Stumpf, M.; Keller, H.-M.; Hase, W. L.; Schinke, R. *J. Chem. Phys.* **1995**, *102*, 5867.
(99) Polik, W. F.; Moore, C. B.; Miller, W. H. *J. Chem. Phys.* **1988**, *89*, 3584.
(100) (a) Andresen, P.; Rothe, E. W. *J. Chem. Phys.* **1985**, *82*, 3634. (b) Schinke, R.; Engel, V.; Andresen, P.; Häusler, D.; Balint-Kurti, G. G. *Phys. Rev. Lett.* **1985**, *55*, 1180.
(101) Vanzee, R. D.; Pibel, C. D.; Butenhoff, T. J.; Moore, C. B. *J. Chem. Phys.* **1992**, *97*, 3235.
(102) Wittig, C. Private communication.

JP952843W